Spectrally resolved electronic energy transfer from silicon nanocrystals to molecular oxygen mediated by direct electron exchange

E. Gross, D. Kovalev, N. Künzner, J. Diener, and F. Koch
Physik-Department E16, Technische Universität München, D-85747 Garching, Germany

V. Yu. Timoshenko
Faculty of Physics, Moscow State M. V. Lomonosov University, 119992 Moscow, Russia

M. Fujii
Department of Electrical and Electronics Engineering, Faculty of Engineering, Kobe University, Rokkodai, Nada, Kobe 657-8501, Japan
(Received 1 April 2003; published 9 September 2003)

We report on a spectroscopic study of electronic energy transfer from excitons confined in silicon nanocrystals to triplet ground-state oxygen molecules, being either physisorbed on the nanocrystal surface or present in the gas phase. The broad photoluminescence spectrum of the nanocrystal assembly probes the transfer of excitation and verifies that nonresonant energy transfer proceeds via multiphonon emission. At low temperatures a small spatial separation of the interacting species and a long lifetime of triplet-state excitons provide the strongest coupling. The energy-transfer time to the first and second excited states of molecular oxygen is in the range of 100 μs and shorter than 3 μs, respectively. Nanocrystals with a chemically modified surface are employed to demonstrate that energy transfer is governed by direct electron exchange. Magneto-optical experiments reveal the importance of the spin orientation of the exchanged electrons for the transfer rate. In the regime of intermediate temperatures (110–250 K) the transfer of excitation to the O_2 dimer is resolved.

DOI: 10.1103/PhysRevB.68.115405 PACS number(s): 33.50.Hv, 71.35.Gg, 73.22.−f

I. INTRODUCTION

One of the most fundamental consequences of electronically coupled systems is the possibility to exchange energy of excitation. Although the intrinsic properties of the isolated species are well understood, an insight into the energy-transfer mechanism due to different types of interactions is difficult to access experimentally. Different frameworks are used to describe the energy transfer being a key process in various scientific fields. It is well known that deep centers in semiconductors give rise to energy levels in the forbidden band gap and act as efficient traps for free carriers and excitons. During the capturing process the energy of electronic excitations in the crystal is transferred to these localized states by multiphonon emission to account for the energy difference.[1–3] Midgap states reduce the quantum yield of luminescence, but the phonon-assisted transfer cannot be resolved spectroscopically due to two reasons: the initial states are well defined by the band edges of the semiconductor, while the individual local environment of a deep center results in a broad energy band of the final states.

On the contrary, in the field of photophysics and photochemistry the transfer of electronic excitation is treated within the concept of photosensitization.[4] If quantum-mechanical selection rules (e.g., spin, parity, and angular momentum) inhibit the efficient direct excitation of a substance by light, an intermediary substance (donor) with optically allowed transitions is employed and subsequent energy transfer to the acceptor molecules occurs. For an efficient transfer of excitation a long lifetime of the donor excited state, the overlap of the donor and acceptor energy levels, and a small spatial separation of the interacting species are essential. To fulfill these demands organic dye molecules in solution are conventionally used as donors. Spin-triplet states of the excited donor assure a slow decay rate. A maximum spectral overlap results from homogeneously broadened energy levels governed by the large vibrational and rotational degree of freedom and collisions with solvent molecules. However, these broadening effects prevent clarification of the detailed process of excitation transfer by means of spectroscopy.

The interest molecular oxygen (MO) has attracted in various scientific fields, e.g., molecular physics and photochemistry, stems from its particular electronic configuration (scheme, Fig. 1). Oxygen molecules in the $^3\Sigma$ ground state (superscript denotes the spin multiplicity) possess two unpaired electrons that are assigned to different atoms and have parallel spin alignment. The resulting spin-triplet state accounts for the paramagnetic properties and the poor chemical reactivity of MO, because the formation of singlet molecules from triplet and singlet reactants is forbidden by the spin selection rule. The lowest excited states ($^1\Delta$, $^1\Sigma$) have singlet nature and arise from an electron redistribution among the orbitals and antiparallel spins. Spin and angular momentum selection rules inhibit an efficient direct optical excitation of the $^1\Delta$ and the $^1\Sigma$ state, lying 0.98 eV and 1.63 eV above the ground state, respectively.[5] This results in long radiative lifetimes of the electric quadrupole ($^1\Delta \rightarrow {}^3\Sigma$) and magnetic dipole ($^1\Sigma \rightarrow {}^3\Sigma$) transitions in isolated oxygen molecules, being 50 min and 7 s, respectively.[5]

Microporous silicon (PSi) is a structural modification of bulk silicon (Si), realized by electrochemical etching of Si wafers. It consists of a Si nanocrystal skeleton and an interconnected pore network with an average structure size of 2–5 nm.[6] Due to quantum confinement effects and a distribution of sizes and shapes of the Si particles, the effective band-gap energies of the nanocrystal assembly range from

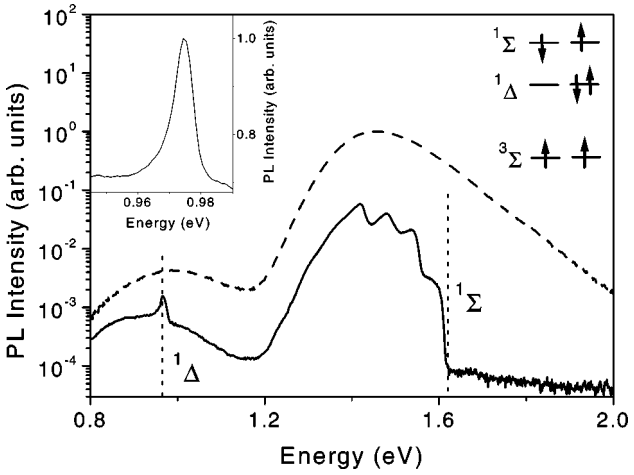

FIG. 1. Emission spectrum of PSi in vacuum (dashed line) and in the presence of adsorbed oxygen molecules (solid line). The spectral positions of excited states ($^1\Delta$, $^1\Sigma$) of MO are indicated. Electronic-spin configurations and spectroscopic labeling of molecular oxygen states are shown. Inset: High-resolution spectrum of the $^1\Delta$ state emission line. $T=5$ K, $E_{exc}=2.41$ eV.

1.12 eV up to 2.5 eV. The optical absorption-emission cycle of Si nanocrystals is characterized by two possible spin configurations of the confined exciton: an optically active spin-singlet state and an optically inactive spin-triplet state, which is lowered in energy due to the electron-hole exchange interaction. Despite a small singlet-triplet splitting being in the meV range,[6] 75% of the excitons reside in the threefold degenerated triplet state even at elevated temperatures. The long lifetime of the excitons is governed by the indirect nature of the optical transition and the corresponding spin selection rules. At cryogenic temperatures only the triplet exciton state is occupied and radiative decay proceeds on a millisecond time scale. At room temperature excitons persist in the triplet state on a time scale comparable to the radiative lifetime of singlet excitons, being 10–100 μs.[6] Thus, the electronic structure of excitons in Si nanocrystals is very similar to that of dye molecules. The morphology of PSi results in a huge accessible internal surface area (up to 1000 m^2/cm^3) that permits a direct contact between the whole Si nanocrystal assembly and molecules present in the interconnected pores. Therefore, PSi meets the main requests on a photosensitizer concerning an efficient transfer of energy.

Here we report on a spectroscopic study of the energy-transfer mechanism in a coupled binary system containing Si nanocrystals and oxygen molecules. Its specific characteristics allow us to combine the above-mentioned concepts, and a detailed, self-consistent description of the transfer process is obtained. Recently, we have shown that due to the overlap of the energy levels of Si nanocrystal assemblies and MO, PSi can be successfully employed in the photosensitized singlet oxygen generation.[7] By adsorption of oxygen molecules on the surface of Si nanoparticles electronic coupling is realized. In this paper we want to demonstate that in this configuration all important physical quantities that determine the energy transfer from excitons confined in Si nanocrystals to MO are experimentally accessible. The infrared emission of the $^1\Delta \rightarrow {}^3\Sigma$ transition verifies the presence of oxygen molecules in the excited state, having a decay time of 500 μs. Upon oxygen adsorption, the initially broad photoluminescence (PL) spectrum of PSi reveals a fine structure that evidences the multiphonon emission during the transfer of excitation. The strong spectral dispersion of the energy-transfer time is in accordance with the phonon-selective transfer process. The difference in the energy-transfer time, being in the range of 100 μs and faster than 3 μs for the $^1\Delta$ and the $^1\Sigma$ state, respectively, is governed by quantum-mechanical selection rules. The dependence of the PL intensity of PSi on the optical excitation power allows us to estimate the average number of adsorbed oxygen molecules per nanocrystal. Controlled modification of the surface termination shows that the energy-transfer mechanism is governed by direct electron exchange. Magnetic-field experiments reveal the importance of the spin orientation of the exchanged electrons for the transfer rate. At elevated temperatures the energy transfer to dimer states of MO and the production of singlet oxygen in the gas phase are demonstrated. The observed dependence of PL quenching on the oxygen gas pressure is discussed in the framework of Langmuir-isotherm molecule adsorption.

II. EXPERIMENTAL DETAILS

PSi layers have been prepared by electrochemical etching of (100) oriented, Boron-doped bulk Si wafers with a resistivity of 50 mΩ cm and 10 Ω cm in a 1:1 by volume mixture of hydrofluoric acid (50 wt% in water) and ethanol.[6] The current density and etching time ranges from 25 mA/cm^2 to 100 mA/cm^2 and from 1 to 10 min, respectively. The thickness of the porous layer varies from 6 μm to 30 μm with a mean nanocrystal size of 2–10 nm, depending on the substrate used.[8] A modification of the chemical composition of the surface layer of the as-prepared nanocrystals is realized by tempering the porous layers at 200 °C in oxygen ambient. The porous layer is mounted on an optical cryostat and experiments are performed either in vacuum or with a given oxygen ambient pressure in the sample chamber. The investigated temperature range is 5–300 K. In the cw PL experiments the sample is excited under normal incidence using an Ar^+-laser (excitation energies 2.41 eV and 2.54 eV) and a tunable Ti-saphire laser (excitation energy range 1.5–1.7 eV). To avoid PL saturation in ordinary PL measurements an excitation intensity less than 10 mW/cm^2 is used. Magneto-optical experiments have been performed in a cryostat equipped with a superconducting solenoid that provides magnetic fields up to 11 T. For excitation of the sample and collection of the emitted light fiber optics has been employed. The dependence of the PL emission on the excitation intensity has been measured using optically thin samples to assure homogeneous excitation of the layer in depth.[9] Time-resolved measurements are carried out with a pulsed, frequency-doubled Nd-YAG(yttrium aluminum garnet) laser (excitation energy 2.33 eV, pulse energy 1 mJ, repetition rate 10 Hz, pulse duration 8 ns, and spot size 5 mm). The spectrally resolved intensity of the emitted light is measured with a monochromator equipped with a charge-coupled device

(detection energy 1.3–2.5 eV) or a nitrogen-cooled Ge detector (detection energy 0.8–1.5 eV). The spectral resolution is 2 meV and all spectra are corrected on the spectral sensitivity of the optical systems. Transients of the infrared and visible emission have been recorded by an InGaAs photomultiplier (100 ns response time) and an S1 photomultiplier (3 μs response time), respectively.

III. RESULTS AND DISCUSSION

A. Energy transfer at cryogenic temperatures

Figure 1 demonstrates the strong interaction of photoexcited Si nanocrystals with oxygen molecules. The low-temperature PL spectrum of PSi measured in vacuum (dashed line) is characterized by a broad, featureless emission band located in the visible region that reflects the wide band-gap distribution of the Si nanocrystal assembly. Intrinsic defects, commonly attributed to unoccupied Si orbitals at the surface of the nanocrystal (dangling bonds), strongly influence the light emission properties. They give rise to broad energy levels within the band gap, and trapping of free carries occurs on a submicrosecond time scale. Thus, nanocrystals having dangling bonds do not contribute to the visible PL but cause a weak infrared emission band due to a small probability of radiative recombination at the defect site.[10]

These emission spectra are drastically modified by the physisorption of oxygen molecules (Fig. 1, solid line). Both emission bands of PSi are quenched and the spectrum exhibits a fine structure. The spectral position of the PL quenching onset and of the narrow infrared emission line coincide with the energies of the $^1\Sigma$-$^3\Sigma$ and $^1\Delta$-$^3\Sigma$ transitions of MO (in the following, the terms $^1\Sigma$ state and $^1\Delta$ state refer to the energy of these transitions). This indicates that these two characteristic energies are entirely relevant to both systems, the Si nanocrystal assembly and MO. Desorption of oxygen molecules leads to a complete recovery of the initial emission properties of PSi which evidences the reversibility of the quenching mechanism.

In the coupled system the triplet-singlet transitions of MO play a role of midgap levels that are externally introduced to the inhomogeneously broadened band-gap distribution of the nanocrystal assembly. The transfer of energy from excitons confined in Si nanocrystals to oxygen molecules is apparent from the almost complete suppression of the PL emission above 1.63 eV and the $^1\Delta$ state emission line (quenching of the infrared emission band will be discussed later). The triplet-triplet annihilation during the transfer process conserves the electronic spin. However, angular momentum conservation is only fulfilled for the energy transfer to the $^1\Sigma$ state, whereas the $^3\Sigma \rightarrow {}^1\Delta$ excitation requires a change of angular momentum ($\Delta L = 2$). The strong coupling of the $^1\Sigma$ state results in a strong PL suppression, while partial quenching occurs for nanocrystals that interact weakly with the $^1\Delta$ state. The back transfer of energy from the $^1\Sigma$ state to Si nanocrystals is inhibited by its fast relaxation either to the $^1\Delta$ state or to the $^3\Sigma$ state,[11] whereas energy transfer from the $^1\Delta$ state is impossible since its energy is below the band gap of bulk Si. We note that for physisorbed oxygen the energies of the infrared $^1\Delta$ emission line (0.973 eV, inset Fig. 1) and of the PL onset (1.619 eV) are lower than those known for gaseous oxygen, being 0.98 eV and 1.63 eV, respectively. The weak van der Waals interaction of adsorbed oxygen molecules with Si surface atoms lowers the energy of the excited states of MO and slightly broadens the transitions.

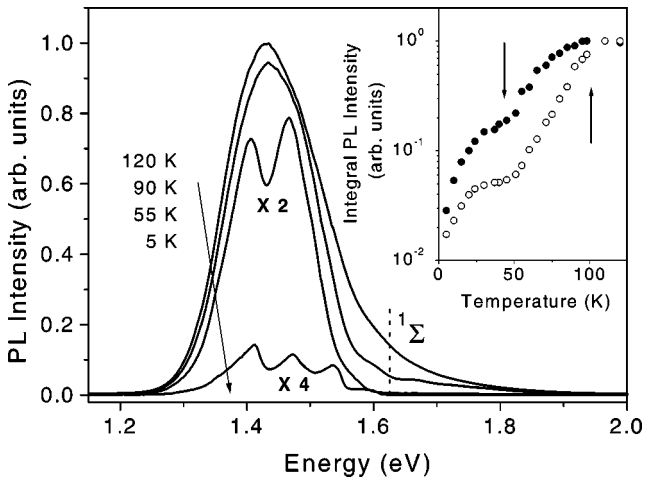

FIG. 2. Temperature dependence of the PL spectrum of PSi in oxygen ambient (pressure of oxygen at $T = 300$ K is 10^{-2} mbar). For better comparison spectra at 55 K and 5 K have been scaled by the indicated multiplication factor. Inset: Integral PL intensity of the PSi emission above (open circles) and below (closed circles) the $^1\Sigma$ state as a function of temperature. Arrows indicate the temperatures where efficient energy transfer is activated.

The efficiency of the energy transfer is governed by the number of oxygen molecules physisorbed on the surface of Si nanocrystals as well as by the exciton lifetime. To separate these two contributions to the strength of PL quenching we measured its temperature dependence (Fig. 2, pressure of oxygen at $T = 300$ K is 10^{-2} mbar). For temperatures above 120 K a large spatial separation between oxygen molecules in the gaseous state and Si nanocrystals inhibits a mutual interaction and the shape of the PL spectrum remains unchanged. Slightly above the bulk condensation temperature of oxygen (90 K), molecule adsorption takes place and efficient PL quenching above the $^1\Sigma$ state is observed. Significant energy transfer to the weakly coupled $^1\Delta$ state requires additionally a long lifetime of the exciton. At temperatures below 55 K the exciton lifetime increases substantially due to the preferential occupation of the triplet exciton state[6] and further quenching of the whole spectrum occurs. The integral PL intensity of the PSi emission above (open circles) and below (closed circles) the $^1\Sigma$ state as a function of temperature is shown in the inset of Fig. 2. In this representation the two distinct onsets, relevant to the adsorption of MO (100 K) and the increase of the exciton lifetime (≈ 50 K), are indicated by arrows.

To investigate the nature of the spectroscopic fine structure, the tunable emission properties of Si nanocrystal assemblies are employed. Different sample preparation procedures[8] are used to vary the size distribution of the Si nanocrystal assembly and shift the luminescence energies from the band gap of bulk Si up to 2.2 eV (Fig. 3, dotted lines). To resolve

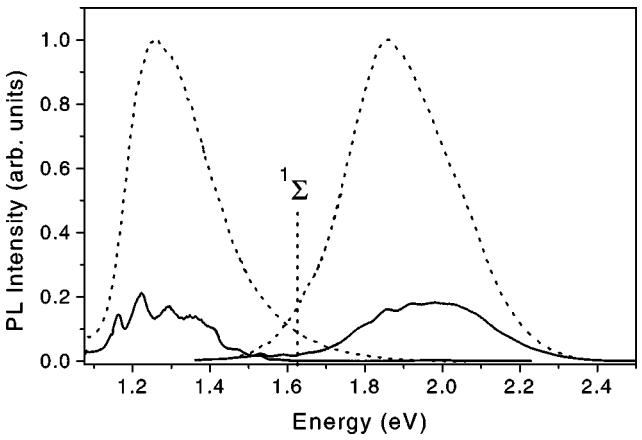

FIG. 3. PL spectra of PSi in vacuum (dotted lines) and with adsorbed oxygen molecules (solid lines). Substrate resistivity and etching current density are 50 mΩ cm, 40 mA/cm^2 (left emission band) and 10 Ω cm, 100 mA/cm^2 (right emission band). $T=5$ K and $E_{exc}=2.54$ eV.

the spectral features above the $^1\Sigma$ state that is strongly coupled to excitons confined in Si nanocrystals, a weak PL suppression has been realized by a low concentration of adsorbed oxygen molecules (Fig. 3, solid lines). The quenched emission spectra reveal a fine structure which is present in the entire probed spectral range and the features have identical spectral positions for samples having different PL bands.

Signatures in the PL of PSi have been previously observed under resonant excitation.[12,13] They have been assigned to momentum-conserving phonons of bulk Si involved in the optical transitions since their spectral position is fixed with respect to the excitation energy. The resonant excitation of the quenched PL (Fig. 4, position of the laser energies is shown by arrows) demonstrates a different behavior. The spectral positions of the features neither depend on excitation energy nor are related to the demarcation energy introduced by the $^1\Sigma$ state of MO. They can be readily seen even at excitation below the energy of the $^1\Sigma$ state.

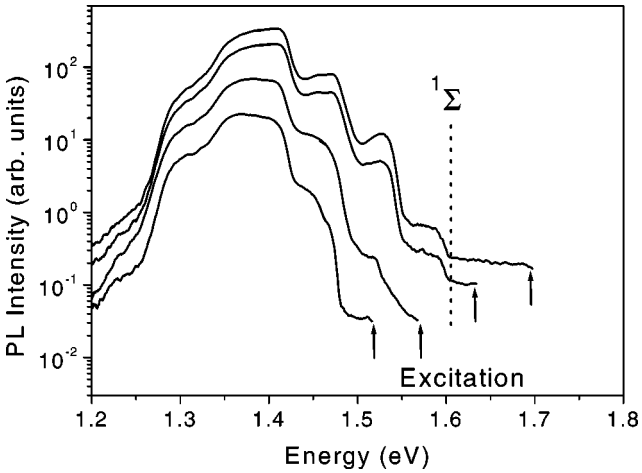

FIG. 4. Resonantly excited PL spectrum of PSi with oxygen molecules adsorbed on the Si nanocrystal surface. Spectral position of the excitation is indicated by arrows. $T=5$ K.

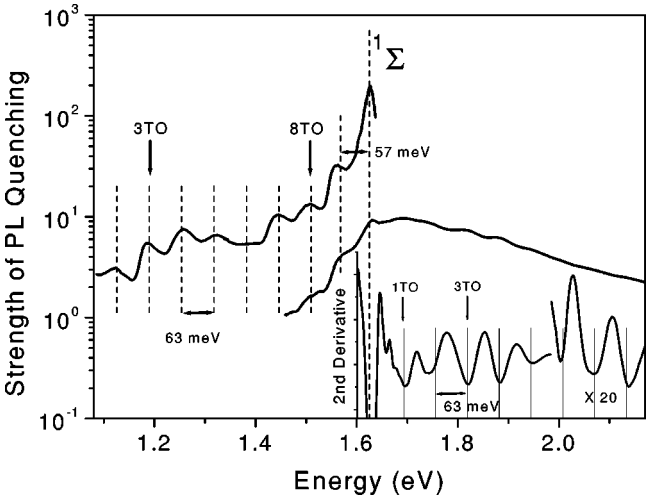

FIG. 5. Spectral dependence of the PL quenching strength of PSi ($T=5$ K). Spectroscopic features, related to multiple TO-phonon emission, are representatively labeled at two spectral positions. Vertical dotted lines are guide for the eye. Inset: Second derivative of the quenching strength curve shown above. For convenient presentation, the data has been partially scaled by the indicated multiplication factor.

As follows from Fig. 3, the exact shape of the quenched PL spectra is defined by the convolution of the ''envelope function,'' i.e., the Si nanocrystal size distribution and the spectral dependence of the coupling strength between excitons and MO. To eliminate the influence of the size distribution on the shape of the quenched PL spectrum we define the strength of quenching as the ratio of the PL intensity measured in vacuum to that measured in quenched condition.[14] Figure 5 demonstrates the results of this procedure for the spectra shown in Fig. 3. To resolve the weak spectral modulation of the curve covering the energy region above the $^1\Sigma$ state its second derivative is used (partial scaling is used for convenient presentation).

The spectral dependence of the PL suppression strength allows a detailed description of the energy-transfer mechanism. Quenching is strongest for nanocrystals having bandgap energies that coincide with the $^3\Sigma$-$^1\Sigma$ transition of MO. Since Si nanocrystals also luminesce 57 meV below their bandgap due to the emission of a momentum-conserving TO phonon,[6] they do not contribute to the PL while transferring the excitation. Therefore, an additional maximum in the quenching strength is observed 57 meV below the $^1\Sigma$ state energy. It is evident from Fig. 5 that nanocrystals whose band gaps do not match resonantly the excitation energies of MO singlet states participate in the energy transfer as well. The excess of the exciton energy with respect to the energies of the $^1\Delta$ and $^1\Sigma$ states is released by the emission of phonons. In Fig. 6 the mechanism of energy transfer from excitons to MO is sketched. Since real electronic states below the nanocrystal band gap are absent, energy dissipation should be governed by multiphonon emission rather than a phonon cascade. This process is most probable for phonons having the highest density of states which in bulk Si are transversal optical phonons being almost at the center of the

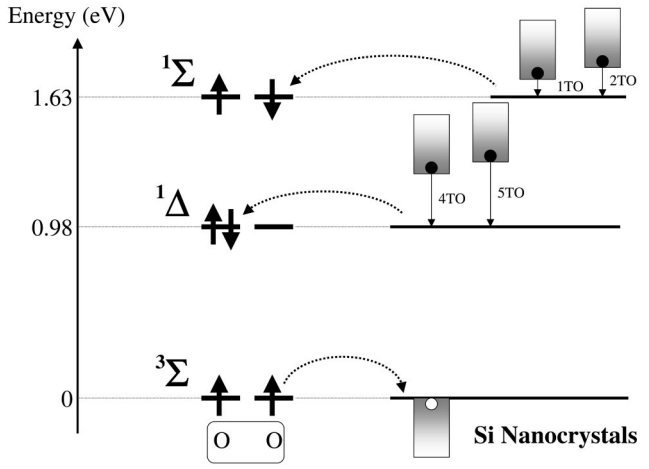

FIG. 6. Energy-level diagram of molecular oxygen and the Si nanocrystal assembly. Principal steps of the energy-transfer process are sketched. Direct electron exchange (dotted arrows) is accompanied by multiphonon emission (solid arrows). Electrons photoexcited in Si nanocrystals are exchanged with electrons belonging to MO. This process results in the formation of singlet MO states and compensation of the holes confined in Si nanocrystals.

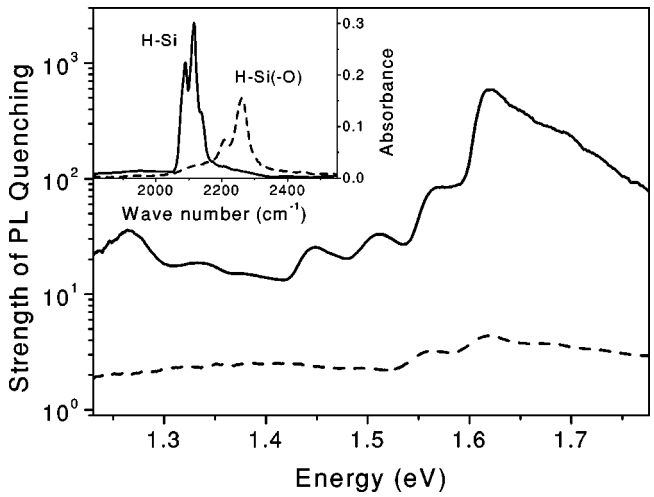

FIG. 7. Spectral dependence of the PL quenching strength of as-prepared (solid line) and oxidized (dotted line) PSi at equal oxygen ambient pressures. $T=5$ K. Inset: Infrared absorption spectrum of the Si-H bond in PSi layers: as-prepared (solid line) and oxidized with backbonded oxygen (dotted line).

Brillouin zone with an energy of 63 meV.[15] If the band-gap energy of Si nanocrystals does not coincide with the excitation energy of a MO singlet state plus an integer number of the energy of those phonons, the additional emission of acoustical phonons is required to conserve the energy. This process has smaller probability and the efficiency of energy exchange is reduced. Consequently, equidistant maxima and minima in the spectral dependence of the quenching strength appear, which experimentally evidences the phonon-assisted energy transfer.[16] The energy-transfer resonances can be spectrally resolved due to a singularity in the phonon density of states.

We would like to mention that multiphonon emission can accompany the exciton recombination in polar semiconductors.[17] Despite strong exciton-phonon coupling the luminescence intensity of phonon replicas drops orders of magnitude with an increasing number of phonons involved in the exciton recombination.[18] In Si the exciton-phonon coupling is weak, but surprisingly, the simultaneous emission of up to eight phonons during the energy transfer to the $^1\Delta$ and $^1\Sigma$ state is detected with comparable probability. To clarify this observation the mechanism of energy transfer has to be considered in detail.

B. Mechanism of energy transfer

Basically, dipole-dipole (Förster transfer[19]) or direct electron exchange (Dexter transfer[20]) coupling can account for the energy transfer from excitons to MO. Since long-range multipole interaction is based on optically allowed transitions of the donor and acceptor, it cannot be applied to the triplet-triplet annihilation of excitons and MO followed by singlet oxygen creation. However, in the electron exchange mechanism these spin restrictions are lifted, and triplet exciton annihilation accompanied by spin-flip excitation of an oxygen molecule is an allowed process.[21] The energy-transfer rate is defined by the spatial overlap of the electronic wave functions of the interacting species and depends exponentially on the donor-acceptor distance.[20] The advantage of our system is that a controlled variation of the donor-acceptor separation is possible by modification of the nanocrystal surfaces. As-prepared PSi exhibits a hydrogen-terminated surface with characteristic absorption lines of the vibrational modes of the Si-H bond (inset of Fig. 7, solid line). Annealing of the porous layers at 200 °C in oxygen ambient introduces a monolayer of backbonded oxygen on the nanocrystal surface, while the hydrogen passivation of the surface is preserved.[22] The chemically modified surrounding of the Si-H bonds shifts the infrared absorption lines to larger wave numbers (inset Fig. 7, dotted line). For oxidized Si nanocrystals the increased spacing between confined excitons and adsorbed oxygen molecules is on the order of double the length of the Si-O bond (3 Å).[23] This critically affects the efficiency of the electron exchange interaction. Contrary to a strong coupling for hydrogen-terminated nanocrystals (Fig. 7, solid line), the PL quenching efficiency is reduced by orders of magnitude if a thin oxide barrier is present (Fig. 7, dotted line) and spectroscopic signatures are only present for the resonant energy transfer to the $^1\Sigma$ state. The degree of spatial overlap of the electronic wave functions of confined excitons and physisorbed MO depends on the size of the Si nanocrystals. This overlap becomes better for smaller nanoparticles and the probability for energy transfer is higher. On the other hand, for smaller nanoparticles a larger number of emitted phonons is required to conserve the energy, which lowers the probability for energy exchange. We believe that the interplay between these two tendencies results in an almost spectrally constant efficiency of the energy transfer.

While the involved transitions are spin forbidden in isolated Si nanocrystals and oxygen molecules they become allowed through exchange interaction. For the energy transfer

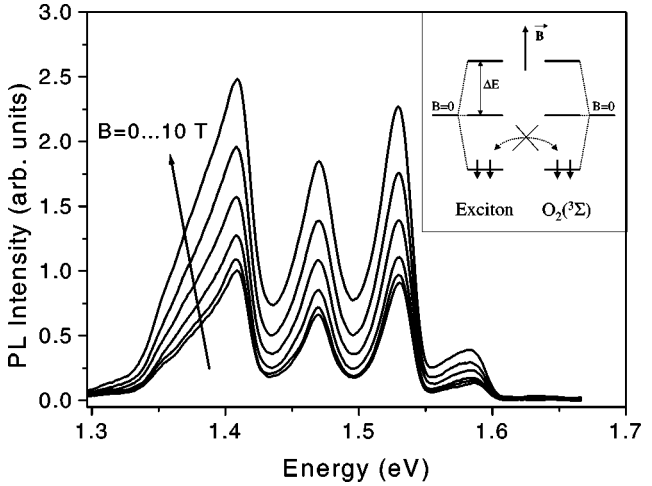

FIG. 8. Quenched PL spectrum of PSi at various strength of magnetic field. $T=10$ K. The magnetic-field increment is equal to 2 T. Inset: Zeeman splitting of triplet-state exciton and $^3\Sigma$ ground state of molecular oxygen. The spin orientations for electrons in the lowest-lying levels are indicated by arrows. Energy transfer from exciton to ground-state MO via electron exchange among these states is prohibited by the conservation of the total magnetic quantum number.

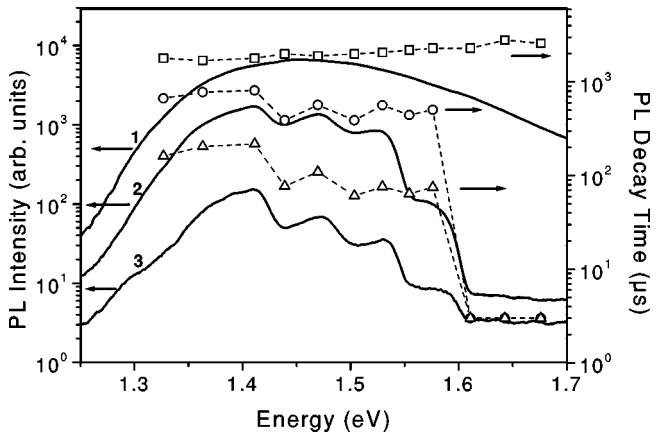

FIG. 9. Emission spectrum of PSi and the corresponding spectral dispersion of the PL decay time for different strengths of quenching. Quenching is absent: 1, squares. Intermediate level of quenching: 2, circles. Strong level of quenching: 3, triangles. $T=5$ K.

to occur the exchanged electrons must have the proper spin orientation to conserve the total magnetic quantum number of the coupled system $M(\text{exciton})+M(\text{MO})$.[24] To demonstrate the influence of spin statistics on the energy-transfer rate we measured the magnetic-field dependence of the PL quenching efficiency (Fig. 8). If no magnetic field is present the energy levels belonging to different M numbers of triplet excitons and the triplet ground state of MO are threefold degenerated and populated with equal probability. Thus, the spin requirements are fulfilled for all excitons and all oxygen molecules, and energy transfer occurs most efficient. A magnetic field introduces a common quantization axis for the spins and the degeneracy is lifted (inset Fig. 8). In general, the number of possible states participating in the electron exchange is reduced[25] and the decreased energy-transfer rate results in a weaker PL quenching. Raising the magnetic field increases the Zeeman splitting ΔE $[g(\text{exciton})\approx g(^3\Sigma)\approx 2]$[26,27] and the occupation number of the thermally populated higher-lying states decreases. At low temperatures a magnetic field results in preferential occupation of ''spin-down'' states for both MO and excitons, while to proceed with energy exchange ''spin-up states'' are required. For magnetic fields of 10 T and a temperature of 10 K the relevant energies $k_BT\approx 0.8$ meV, $\Delta E\approx 1.1$ meV are comparable, and a significant reduction of the PL quenching is observed. For the spectral region above the $^1\Sigma$ state the high PL quenching level prevents the observation of magnetic-field effects within our experimental detection sensitivity.

C. Dynamics of energy transfer

The dynamics of the energy-transfer is deduced from the modified PL decay characteristics of Si nanocrystals in the presence of adsorbed oxygen molecules. The energy-transfer time from one Si nanocrystal to a single oxygen molecule is not accessible experimentally, since a large number of nanocrystals contribute to the PL at a certain emission energy. Though the concentration of physisorbed MO can be varied, it is subjected to statistical fluctuations and the absolute number of artificially introduced surface defects cannot be determined. The emission spectra of PSi at different suppression levels and the corresponding PL decay times τ_D are shown in Fig. 9. In the absence of oxygen adsorption (spectrum 1), τ_D (squares) is equal to the radiative lifetime of excitons τ_r and is on a millisecond time scale,[6] independent on the emission energy. Oxygen molecules attached to the nanocrystal surface present a nonradiative decay channel for excitons due to energy transfer. Suppression of the emission intensity (spectrum 2) is accompanied by a significant decrease of the PL decay time (circles). The spectral dispersion of τ_D follows the shape of the quenched spectrum and the shortest τ_D is observed for nanocrystals that transfer their excitation most efficiently. The determination of the fast PL decay time above the $^1\Sigma$ state energy is limited by the time resolution of the experimental setup, being 3 μs. Increasing the concentration of adsorbed oxygen molecules results in a stronger PL suppression (spectrum 3) and a further decrease of τ_D (triangles).

For a particular level of quenching the time of energy-transfer τ_{ET} is calculated according to the relation $\tau_D^{-1}=\tau_r^{-1}+\tau_{ET}^{-1}$. In the regime of the strongest suppression τ_{ET} for the $^1\Delta$ and $^1\Sigma$ states is 50–100 μs and <3 μs, respectively. A uniform concentration of oxygen molecules for all nanocrystals would result in a quenching strength that scales as τ_r/τ_D. Obviously, this simple relation is not valid. A decay time longer than that expected from the suppression level is observed due to statistical fluctuations of the oxygen concentration: while mainly the slowest emission from nanocrystals with a small number of oxygen molecules adsorbed on the surface contributes to the PL decay, the quenched spectrum reflects the response of all nanocrystals.

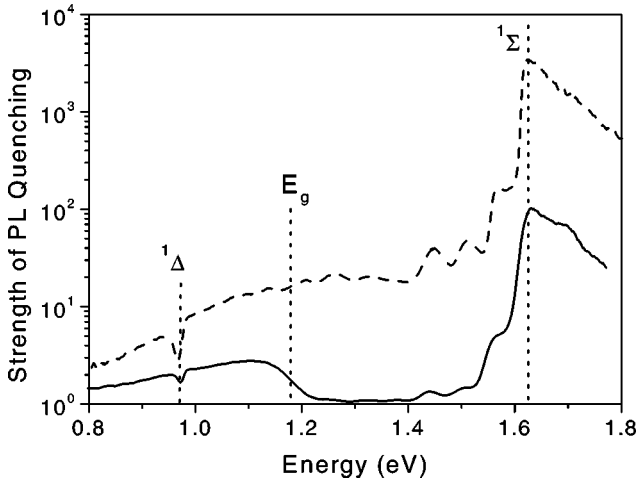

FIG. 10. Spectral dependence of the quenching strength of PSi emission in the weak (solid line) and strong (dashed line) suppression regimes. Spectral positions of the excited states of MO ($^1\Delta$, $^1\Sigma$) and of the bulk Si band gap (E_g) are indicated. $T=5$ K.

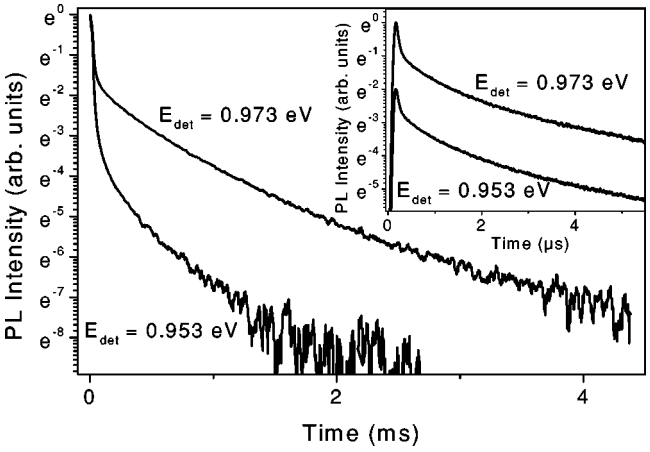

FIG. 11. Transients of the $^1\Delta$ state relaxation and the dangling-bond emission decay, detected at 0.973 eV and 0.953 eV, respectively, for a PSi layer with adsorbed oxygen molecules. Inset: Time-resolved dangling-bond emission of a PSi layer in vacuum. $T=5$ K.

The infrared emission from PSi is obviously also affected by the adsorption of oxygen (see Fig. 1). To clarify the underlying process the spectral dependence of the quenching strength for different suppression levels has been measured (Fig. 10). Because quenching of the dangling-bond emission band occurs even below the $^1\Delta$ state of MO (dashed line), the transfer of excitation from occupied defect states to oxygen molecules can be excluded due to energy conservation. Instead, the competition of the nonradiative decay channels for photogenerated excitons, i.e., MO activation and capturing of carriers to dangling bonds, has to be taken into account. If the capture time and the energy-transfer time are of comparable value, the number of charged midgap states and consequently the infrared emission intensity of the defect band should be reduced. This relation is fulfilled for nanocrystals with a sufficiently large effective band gap (above 1.63 eV), where excitons are strongly coupled to the $^1\Sigma$ state. These nanocrystals mainly contribute to the high-energy part of the defect luminescence band due to their large confinement energy.[10] To confirm the interplay between the excitation of MO and the suppression of the dangling-bond emission the regime of weak quenching has been realized (solid line). Coupling to the $^1\Delta$ state is negligible, while significant energy transfer to the $^1\Sigma$ state is still present. The suppression of the infrared emission band is most efficient at higher energies and can be observed at any level of quenching of the visible PL band. Therefore, we conclude that energy exchange between excitons and MO competes with the capture of carriers to defect states. This implies that even nonluminescing nanocrystals having surface defects can contribute to singlet oxygen activation. Contrary to quenching of the visible PL band, broadening of the defect levels inhibits the observation of phonon replicas.

The relevant time scales of the infrared emission are determined from time-resolved measurements. Inset of Fig. 11 shows the transients of the dangling-bond emission for PSi in vacuum detected at 0.953 eV and 0.973 eV (transients are separated vertically for better comparison). The rise time coincides with the response time of our setup (≈ 100 ns) and yields an upper limit for the time of carriers capture to defect states. The nonexponential decay proceeds on a microseconds time scale and does not vary with emission energy. In the presence of adsorbed oxygen molecules the relaxation kinetics of the $^1\Delta$ state is observed (Fig. 11, detection energy 0.973 eV). The initial fast decay is attributed to the dangling-bond PL background, which has been separately measured at a detection energy of 0.953 eV. This inhibits the observation of the PL rise time of the $^1\Delta$ state. The slow component, having a lifetime of $\tau_{lt}(^1\Delta)\approx 500\ \mu$s, accounts for the dipole-forbidden $^1\Delta \rightarrow {}^3\Sigma$ transition and falls in the range of previously reported values (3 μs–300 ms).[28] Previous experimental observations confirm that each exciton which is lost for the radiative emission process necessarily generates an oxygen molecule in its excited state. This allows us to estimate the radiative quantum yield $\eta(^1\Delta)$ of the $^1\Delta$ state. The ratio of the integral intensity of the $^1\Delta$ emission line to the overall intensity loss of the excitonic emission (see Fig. 1) results in $\eta(^1\Delta)\approx 7\times 10^{-5}$. The perturbing interaction with Si nanocrystals shortens the radiative lifetime of the $^1\Delta$ state $\tau_r(^1\Delta)$ with respect to isolated oxygen molecules (50 min) and $\tau_r(^1\Delta)\approx 7$ s is obtained using the simple relation $\eta(^1\Delta)=\tau_{lt}(^1\Delta)/\tau_r(^1\Delta)$.

In Si nanocrystal assemblies the number of generated excitons at low temperatures is limited due to their long lifetime and the high efficiency of nonradiative Auger processes.[29] The PL intensity of PSi layers in vacuum increases linearly with the excitation intensity up to ≈ 20 mW/cm^2 (Fig. 12, squares). At higher excitation intensities an occupation of Si nanocrystals by two electron-hole pairs can be achieved, and nonradiative Auger recombination results in a saturation behavior of the emission intensity. Upon oxygen adsorption, the emission intensity of PSi is suppressed and shows a quite different dependence on the optical excitation power. In the steady-state conditions for the coupled system (Si nanocrystals–oxygen molecules), a certain fraction of adsorbed oxygen molecules persists in the

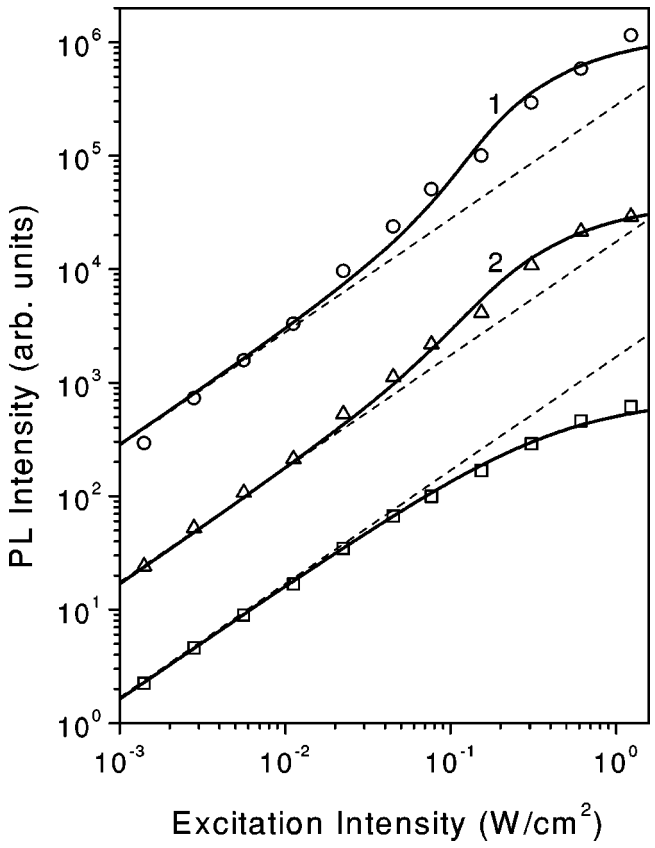

FIG. 12. PL intensity of PSi in vacuum (squares, $E_{Det}=1.47$, 1.5 eV) and with adsorbed oxygen molecules (triangles, $E_{Det}=1.47$ eV; circles, $E_{Det}=1.5$ eV) vs excitation intensity. $E_{Det}=1.47$ eV corresponds to weaker and $E_{Det}=1.5$ eV to stronger coupling between excitons and MO. Solid lines are solutions of rate equations with $\tau_r=1.5$ ms, $\sigma=10^{-15}$ cm^2, and 1, $\tau_{ET}=130$ μs, $\tau_{lt}=4$ ms; 2, $\tau_{ET}=250$ μs, $\tau_{lt}=4$ ms. The datasets are arbitrarily scaled for clarity. Dashed lines are linear power laws. $T=5$ K, $E_{exc}=2.41$ eV.

$^1\Delta$ excited state because of the finite relaxation rate of the $^1\Delta \rightarrow {}^3\Sigma$ transition. This group of molecules does not contribute to PL quenching and acts as a bottleneck for the energy transfer. Raising the excitation intensity increases the occupation number of excited oxygen molecules and PL quenching becomes less efficient. Therefore, a superlinear growth of the emission intensity is obtained at intermediate pump intensities.

The response of the coupled system on the excitation power can be well described by a simple set of rate equations

$$\dot{N}_0 = -N_0\sigma I_{exc} + \frac{N_1}{\tau_r} + \frac{N_1 n_g}{\tau_{ET}}, \quad \dot{n}_g = -\frac{N_1 n_g}{\tau_{ET}} + \frac{n_e}{\tau_{lt}} \quad (1)$$

$$N = N_0 + N_1, \quad n = n_g + n_e,$$

where N_0, N_1 are the numbers of nanocrystals containing 0 and 1 exciton, respectively, N is the total number of nanocrystals, τ_r is the radiative exciton lifetime, σ is the optical absorption cross section of a nanocrystal, and I_{exc} is the areal flux density of exciting photons. n_g and n_e denote the number of oxygen molecules being in the ground and the $^1\Delta$ excited state, respectively, n is the total number of oxygen molecules, τ_{lt} is the lifetime of the $^1\Delta$ state, and τ_{ET} is the time of energy transfer from one exciton to one oxygen molecule. Neglecting higher exciton occupation numbers of a single nanocrystal in the present notation implicitly accounts for the fast nonradiative Auger processes whose typical times are in the nanosecond range.[29] The rate equations describing the emission properties of Si nanocrystals in vacuum are deduced by setting $n=n_g=n_e=0$. The PL intensity of the nanocrystal ensemble I_{PL} is obtained from the steady-state solution of the equations and the relation $I_{PL}=N_1/\tau_r$. The time constants used in the model have been measured whereas σ is known from literature.[30]

The experimentally determined energy-transfer time corresponds to a particular quenching level, i.e., a certain amount of adsorbed oxygen molecules on one nanocrystal. Therefore, for a correct evaluation of the equations only one nanocrystal is considered ($N=1$) and all adsorbed oxygen molecules are treated as a single quenching system ($n=1$). Using the notation τ_{ET} in the rate equations is the measured energy-transfer time. The model takes into account that the quenching system being in the excited state is lost from the quenching process unless it relaxes to the ground state. Thus, τ_{lt} in the equations is not the measured decay time of the $^1\Delta$ state, but a longer time that is scaled with the number of adsorbed oxygen molecules per nanocrystal. The solutions of the equations according to this procedure (Fig. 12, solid lines) coincide well with the measurement. The best fit to the experimental data can be achieved using $\tau_{lt}=4$ ms. This allows us to estimate the mean number of adsorbed oxygen molecules per nanocrystal to be 8.[31] The deviation from the linear regime depends on the detection energy and is stronger for nanocrystals that transfer the excitation faster. Since MO introduces an additional decay channel for excitons, the PL saturation threshold is increased by one order of magnitude compared to PSi layers in vacuum.

Similar considerations applied to the energy transfer to the $^1\Sigma$ state allow us to clarify its relaxation channel. It is well established that the $^1\Sigma$ state is nonradiatively deactivated on a subnanoseconds time scale.[11] However, whether the decay to the $^3\Sigma$ ground state proceeds directly or via the long-living $^1\Delta$ state is still under discussion.[28] If the $^1\Delta$ state is involved as an intermediate level during relaxation, the energy transfer to MO should already be saturated at low excitation intensities due to its fast occupation. Consequently, the PL emission intensity above the $^1\Sigma$ state demarcation energy should strongly rise when the excitation power is increased. On the contrary, according to our observations the PL emission remains completely suppressed up to the highest excitation intensities used (2 W/cm^2), which evidences that the $^1\Sigma$ state mainly relaxes directly to the $^3\Sigma$ state. Therefore, despite a fast energy transfer to the $^1\Sigma$ state ($\tau_{ET}<3$ μs) the main fraction of oxygen molecules adsorbed on small nanocrystals persists in the ground state and efficiently contributes to the PL quenching above 1.63 eV.

D. Energy transfer at elevated temperatures

Spectroscopic experiments at cryogenic temperatures allow us to clarify the details of the energy-transfer mecha-

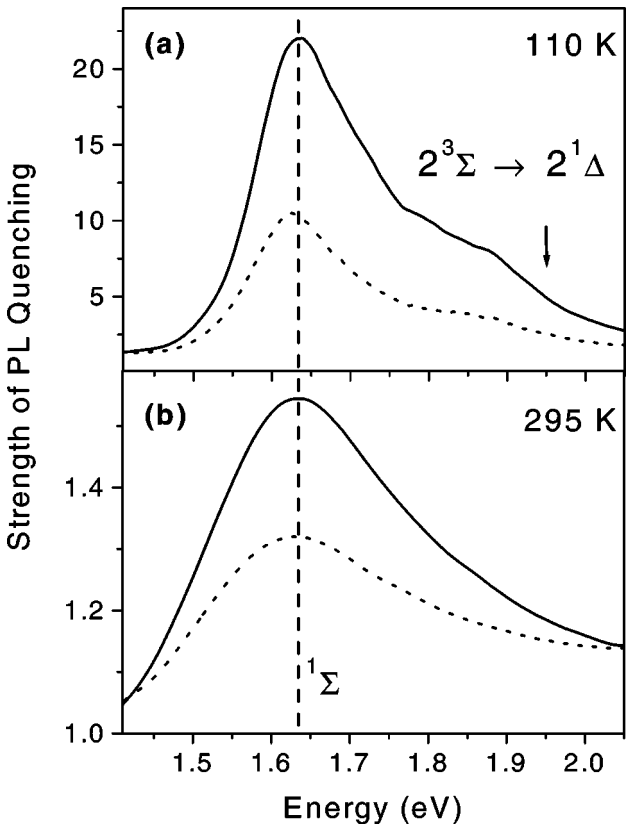

FIG. 13. Spectral dependence of the quenching strength of PSi emission in the ambient of oxygen gas. (a) $T=110$ K, 100 mbar (solid line), 2 mbar (dotted line). (b) $T=295$ K, 1 bar (solid line), 100 mbar (dotted line). The energy positions of the $^1\Sigma$ state and of the $(O_2)_2$ transition are indicated.

nism. However, of most practical interest is the generation of MO in its excited states in the gaseous form at elevated temperatures due to the important role of singlet oxygen in photochemical reactions.[32] The suppression of the PL of PSi in the ambient of different gas pressures of oxygen is evident from Fig. 13. Contrary to cryogenic temperatures, the presuppositions for an optimal interaction are not fulfilled. A small spatial separation is realized only during the short time of collisions between oxygen molecules and the nanocrystal surface. Additionally, the exciton lifetime and the occupation number of the spin-triplet state of the exciton decrease with rising temperature.[6] Therefore, a weaker PL suppression that scales with the collision rate, i.e., the gas pressure, occurs, and the energy transfer to the $^1\Sigma$ state is characterized by a broad spectral resonance. At intermediate temperatures ($T=110$ K) a second quenching band in the spectral region of ≈ 1.75–1.95 eV is observed, which becomes better pronounced with increasing oxygen concentration [Fig. 13(a)]. We attribute it to the energy transfer from excitons confined in Si nanocrystals to the oxygen dimer $(O_2)_2$. The O_2 dimer is known as a complex of ground-state oxygen molecules induced by weak van der Waals interaction. The discrete electronic transition in $(O_2)_2$ corresponding to the $2^3\Sigma \rightarrow 2^1\Delta$ transformation occurs at 1.95 eV (indicated by an arrow) and is thermally and collisionally broadened in the gas phase.[33,34] The $(O_2)_2$ related quenching band in the spectral dependence of the PL quenching strength has an energy below 1.95 eV. We believe that the difference in energy is governed by the physisorption energy of oxygen molecules. Excitation of the bound complex involves spin-conserving electron exchange among the two $^3\Sigma$ states, whereas the exciton provides the energy to activate the process. Consequently, the PL of PSi is quenched in the considered spectral range and energy transfer to the dimer state is enhanced at higher pressures due to an increased probability of $(O_2)_2$ formation. Due to thermal dissociation of the complex [dissociation energy[35] of $(O_2)_2 \approx 10$ meV] a continuous decrease of the dimer related quenching band has been observed while the temperature is increased. For temperatures higher than 250 K the energy transfer to $(O_2)_2$ cannot be resolved spectroscopically.

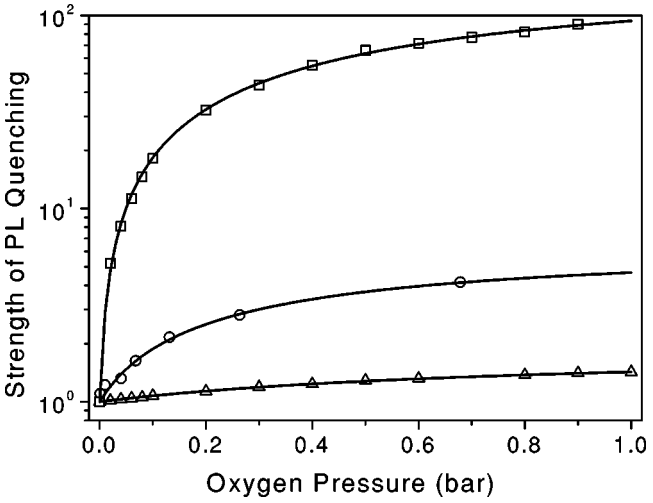

FIG. 14. Dependence of the PL quenching strength, detected at 1.63 eV, on the oxygen gas pressure at different temperatures. Squares: 120 K; circles: 200 K; and triangles: 300 K. Solid lines are calculated pressure dependencies according to Langmuir isotherms for molecule adsorption.

The dependence of the quenching strength detected at 1.63 eV on the oxygen ambient pressure at different temperatures is shown in Fig. 14. It is well described by the Langmuir approach for molecule adsorption on a surface,[36] that considers the dynamic equilibrium between the rate of adsorption and desorption:

$$Q^{-1}=\frac{I_{O_2}}{I_{vac}}=1-A\theta, \quad \theta=\frac{KP}{1+KP}, \tag{2}$$

where Q denotes the strength of quenching, I_{O_2} and I_{vac} are the PL intensities of PSi in the ambient of oxygen and vacuum, respectively, and θ is the fraction of surface covered by oxygen molecules. K is the equilibrium constant, and a measure of the number of adsorbed molecules, P is the oxygen gas pressure, and A is a constant that accounts for the probability of energy transfer to the adsorbed molecules. The best agreement between the experimental data and theoretical predictions (Fig. 14, solid lines) has been found for the following parameters: $T=120$ K:$K=193$ bar^{-1}, $A=0.99$; $T=200$ K:$K=12$ bar^{-1}, $A=0.85$; and $T=300$ K:K

$=1.7\ \mathrm{bar}^{-1}$, $A=0.48$. As expected, in the entire pressure range a decrease of the temperature increases the mean number of adsorbed molecules and enhances the efficiency of energy transfer. The stationary concentration of singlet oxygen is a product of its generation rate and the collisional deactivation rate. Because both quantities are rising with oxygen ambient pressure, further investigations are required to determine the optimal conditions for the highest steady-state concentration of singlet oxygen.

IV. SUMMARY

We presented a spectroscopic study of the energy transfer from excitons confined in Si nanocrystals to oxygen molecules. The strongest coupling among the interacting species is present at cryogenic temperatures, where oxygen molecules are physisorbed on the nanocrystal surface. PL quenching of the nanocrystal assembly and the simultaneous occurrence of the infrared emission line due to relaxation of the $^1\Delta$ state of MO evidences the energy transfer. Its high efficiency is favored by the broad energy spectrum of excitons and their long lifetime. The mechanism of energy transfer is controlled by direct electron exchange, as indicated by the spectral dependence of the PL quenching and magnetic-field measurements. Time-resolved experiments allow us to determine the energy-transfer rate from excitons to MO, which is governed by quantum-mechanical selection rules. The large internal surface area and the open nanostructure of PSi layers are crucial for the energy transfer, i.e., singlet oxygen generation, in the gaseous phase at elevated temperature. Due to the remarkable photosensitizing properties of Si nanocrystal assemblies they are promising candidates for catalysts involved in a variety of photochemical reactions.

ACKNOWLEDGMENTS

This work was supported by Industrial Technology Research Grant Program in 2002 from New Energy and Industrial Technology Development Organization (NEDO), Japan and Deutsche Forschungsgemeinschaft (Grant No. KO 1966/5-1). V.Y.T. is grateful to the Alexander von Humboldt Foundation. We would like to thank S. Hayashi, K. Tsuchihashi, and M. Ushui for useful discussions.

[1] V. N. Abakumov, V. I. Perel, and I. N. Yassievich, in *Nonradiative Recombination in Semiconductors*, edited by V. M. Agranovich and A. A. Maradudin, *Modern Problems in Condensed Matter Science*, Vol. 33 (North-Holland, Amsterdam, 1991).

[2] S. T. Pantelides, *Deep Centers in Semiconductors* (Gordon and Breach Science, London, 1986).

[3] A. M. Stoneham, *Theory of Defects in Solids* (Oxford University Press, Oxford, 1975).

[4] J. F. Rabeck, *Photochemistry and Photophysics* (CRC Press, Boca Raton, 1990).

[5] P.H. Krupenie, J. Phys. Chem. Ref. Data **1**, 423 (1972).

[6] A.G. Cullis, L.T. Canham, and P.D.J. Calcott, J. Appl. Phys. **82**, 909 (1997).

[7] D. Kovalev, E. Gross, N. Künzner, F. Koch, V.Yu. Timoshenko, and M. Fujii, Phys. Rev. Lett. **89**, 137401 (2002).

[8] G. Polisski, H. Heckler, D. Kovalev, M. Schwarzkopff, and F. Koch, Appl. Phys. Lett. **73**, 1107 (1998).

[9] D.I. Chepic, A.L. Efros, A.I. Ekimov, M.G. Ivanov, V.A. Kharchenko, I.A. Kudriavtsev, and T.V. Yaseva, J. Lumin. **47**, 113 (1990).

[10] O. Bisi, S. Ossicini, and L. Pavesi, Surf. Sci. Rep. **38**, 1 (2000).

[11] R. Schmidt and M. Bodesheim, J. Phys. Chem. A **102**, 4769 (1998).

[12] T. Suemoto, K. Tanaka, A. Nakajima, and T. Itakura, Phys. Rev. Lett. **70**, 3659 (1993).

[13] P.D.J. Calcott, K.J. Nash, L.T. Canham, M.J. Kane, and D. Brumhead, J. Lumin. **57**, 257 (1993).

[14] PL spectra have been measured using high energy of excitation to assure equally efficient excitation of all Si nanocrystals in the ensemble.

[15] W. Weber, Phys. Rev. B **15**, 4789 (1977).

[16] Figure 5 evidences PL quenching at ≈ 1.4 eV but a maximum in the strength of quenching is not resolved. This is due to the presence of a remnant weak narrow PL band located at ≈ 1.4 eV, resolved in additional time-delayed PL measurements. The radiative recombination between an electron belonging to the O_2^- complex and a hole confined in a Si nanocrystal is one of the possible processes resulting in this PL band.

[17] J. Conradi and R.R. Haerig, Phys. Rev. Lett. **20**, 1344 (1968).

[18] S. Permogorov, in *Excitons*, edited by V. M. Agranovich and A. A. Maradudin, *Modern Problems in Condensed Matter Science*, Vol. 2 (North-Holland, Amsterdam, 1982).

[19] T. Förster, Ann. Phys. (N.Y.) **2**, 55 (1948).

[20] D.L. Dexter, J. Chem. Phys. **21**, 836 (1953).

[21] A. Damjanovic, T. Ritz, and K. Schulten, Phys. Rev. E **59**, 3293 (1999).

[22] P. Gupta, V.L. Colvin, and S.M. George, Phys. Rev. B **37**, 8234 (1988).

[23] *CRC Handbook of Chemistry and Physics*, 78th ed. edited by D. R. Linde (CRC Press, New York, 1998).

[24] Y. Tanabe and K. Aoyagi, in *Excitons*, edited by V. M. Agranovich and A. A. Maradudin, *Modern Problems in Condensed Matter Science*, Vol. 2 (North-Holland, Amsterdam, 1982).

[25] D.R. Kearns, and A.J. Stone, J. Chem. Phys. **55**, 3383 (1971).

[26] H. Heckler, D. Kovalev, G. Polisski, N.N. Zinov'ev, and F. Koch, Phys. Rev. B **60**, 7718 (1999).

[27] G. Berden, R. Engeln, P.C.M. Christianen, J.C. Maan, and G. Meijer, Phys. Rev. A **58**, 3114 (1998).

[28] F. Wilkinson, W.P. Helman, and A.B. Ross, J. Phys. Chem. Ref. Data **22**, 113 (1993).

[29] C. Delerue, M. Lannoo, G. Allan, E. Martin, I. Mihalcescu, J.C. Vial, R. Romestain, F. Müller, and A. Bsiesy, Phys. Rev. Lett. **75**, 2228 (1995).

[30] D. Kovalev, J. Diener, H. Heckler, G. Polisski, N. Künzner, and F. Koch, Phys. Rev. B **61**, 4485 (2000).

[31] The average number of oxygen molecules adsorbed on one nano-

crystal can also be deduced from estimates based on Poisson statistics. Here we assume that due to the fast energy-transfer to the $^1\Sigma$ state one physisorbed oxygen molecule on the nanocrystal surface is sufficient to quench its PL completely. Taking into account a PL suppression level of 10^3 at 1.63 eV results in a mean number of adsorbed molecules per nanocrystal of ≈ 7. This implies a probability of 10^{-3} for having no molecule adsorbed on the nanocrystal surface.

[32] N. J. Turro, *Modern Molecular Photochemistry* (Benjamin/Cummings, Menlo Park, CA, 1978).

[33] A. Campargue, L. Biennier, A. Kachanov, R. Jost, B. Bussery-Honvault, V. Veyret, S. Chussary, and R. Bacis, Chem. Phys. Lett. **288**, 734 (1998).

[34] J. Goodman, and L.E. Bruce, J. Chem. Phys. **67**, 4408 (1977).

[35] J. O. Hirschfelder, C. F. Curtiss, and R. B. Bird, *Molecular Theory of Gases and Liquids* (Wiley, New York, 1954).

[36] I. Langmuir, J. Am. Chem. Soc. **38**, 2221 (1916).